

Heavy LSP Supersymmetry

TAOLI CHENG^{1,3*}, JINMIAN LI^{1†}, TIANJUN LI^{1,2‡}

¹ *State Key Laboratory of Theoretical Physics, Institute of Theoretical Physics, Chinese Academy of Sciences, Beijing 100190, P. R. China*

² *School of Physical Electronics, University of Electronic Science and Technology of China, Chengdu 610054, P. R. China*

³ *Max-Planck-Institut für Physik (Werner-Heisenberg-Institut),
Föhringer Ring 6, 80805 München, Germany*

Abstract

To escape the current LHC supersymmetry (SUSY) search constraints while preserve the naturalness condition, we propose the heavy Lightest Supersymmetric Particle (LSP) SUSY. To show why the heavy LSP SUSY can avoid all the LHC constraints, we define an energy scale measure P to estimate the typical energy of a process, and present the detailed kinematic analyses both analytically and numerically. With the distributions of the collider observables related to P , we can also derive the shape of cut efficiency approximately for an experimental analysis. Especially, all the current LHC SUSY search constraints can be evaded if the LSP mass is around 600 GeV or higher. In the Minimal Supersymmetric Standard Model (MSSM), we find that the heavy LSP SUSY does not induce more fine-tuning than Higgs boson mass. We systematically study the viable parameter space for heavy LSP SUSY, and present four benchmark points which realize our proposal concretely.

*ctl@itp.ac.cn

†jmli@itp.ac.cn

‡tli@itp.ac.cn

1 Introduction

The Standard Model (SM)-like Higgs boson with mass m_h around 125 GeV was discovered at the first run of the LHC in July 2012 [1, 2]. Such a large Higgs boson mass requires the multi-TeV top squarks with small mixing or TeV-scale top squarks with large mixing in the Minimal Supersymmetric SM (MSSM) [3–5]. Moreover, the null results for the LHC supersymmetry (SUSY) searches have given strong constraints on the pre-LHC viable parameter space. For instance, the gluino mass $m_{\tilde{g}}$ should be heavier than about 1.7 TeV if the first two-generation squark mass $m_{\tilde{q}}$ is around the gluino mass $m_{\tilde{q}} \sim m_{\tilde{g}}$, and heavier than about 1.3 TeV for $m_{\tilde{q}} \gg m_{\tilde{g}}$ [6, 7]. Because the supersymmetric particles (sparticles) should be above TeV scale for the ordinary SUSY scenarios [8], the little hierarchy problem [9, 10] and naturalness problem [11] in SUSY models are aggravated.

Many new models have been proposed to increase the Higgs boson mass. For example, in the singlet or triplet extended MSSM [12–16], the SM-like Higgs boson mass can get an extra tree-level contribution proportional to the trilinear coupling in superpotential. And the mixing between the SM-like Higgs boson and another lighter Higgs field can help lifting the SM-like Higgs boson mass via their mass matrix diagonalization. Because the large loop contributions from top-stop sector is not needed, the stops can indeed be light as well.

To evade the current LHC SUSY search constraints, we can consider the following SUSY scenarios

- **R-parity violation** [17] If R-parity is broken in SUSY models, the large \cancel{E}_T requirement in most of SUSY searches is no longer fulfilled. So, the corresponding strong bounds can be avoided. However, the bounds may remain strong when the R-parity breaking superpotential violates lepton number but preserves baryon number [18, 19].
- **Compressed SUSY** [20, 21] When the sparticles and Lightest Supersymmetric Particle (LSP) have degenerate masses, all decay final states of the SUSY events will be too soft to be detected at LHC. In this case, the events can only be probed when a hard Initial State Radiated (ISR) jet recoils against the sparticle system. Many studies have been carried out for stop [22, 23], sbottom [24], gluino [25], and higgsino [26, 27].
- **Displaced SUSY** [28] If a neutral sparticle has a decay length around \sim mm, the momentum of its decay products will not point to the primary vertex of the event. So, there will be a great possibility that these decay products can not be properly reconstructed. As a result, there will be less charged tracks associated to the event, which reduce the trigger efficiency.
- **Stealth SUSY** [29] In contrast to the compressed SUSY scenario, the missing transverse energy (E_T^{miss}) is small because of the softness of the invisible particle itself, not because of the cancellation of two invisible particle energies. And then even the ISR jet is not able to produce large E_T^{miss} .
- **“Double-invisible” SUSY** [30, 31] If sparticles have multi-body decays into more than one invisible particles, both the visible and invisible energy in the final states will be soften.

Before we propose the heavy LSP SUSY, let us explain the fine-tuning in SUSY models and the LHC SUSY search constraints first. In the Minimal Supersymmetric Standard Model (MSSM), the Higgs boson mass is bounded by Z boson mass at tree level, and the top-stop corrections can lift it to the observed value $m_h \sim 125$ GeV as follows

$$m_h^2 \simeq m_Z^2 \cos(2\beta) + \frac{3m_t^4}{4\pi^2 v^2} \left(\log\left(\frac{M_S^2}{m_t^2}\right) + \frac{X_t^2}{M_S^2} \left(1 - \frac{X_t^2}{12M_S^2}\right) \right), \quad (1)$$

where $M_S = \sqrt{m_{\tilde{t}_1} m_{\tilde{t}_2}}$, $X_t = A_t - \mu/\tan\beta$, $v = 174$ GeV, and m_t is the running top mass at m_t scale. In the large $\tan\beta$ limit, the radiative corrections are required as large as tree-level contribution

$$\delta_t^2 \simeq (125)^2 - (91)^2 \simeq 7.34 \times 10^3. \quad (2)$$

If the logarithmic term gives the dominant contribution, the average stop mass M_S will be required above TeV scale. However, in the maximal mixing scenario [32] with $X_t \simeq \sqrt{6}M_S$, the third term can give dominant contribution to Higgs boson mass without very heavy stop. Natural SUSY strongly favours this region. From Eq. (1), we have

$$\frac{3m_t^4}{4\pi^2 v^2} \times \frac{X_t^2}{M_S^2} \left(1 - \frac{X_t^2}{12M_S^2}\right) \sim \frac{3m_t^4}{4\pi^2 v^2} \times 3 \sim 7 \times 10^3, \quad (3)$$

which just satisfies the condition in Eq. 2. Then the top-stop sector is mainly constrained by the absence of the color breaking vacuum which usually means $|X_t/M_S| \lesssim \sqrt{6}$ and the requirement of the electric and color neutral LSP ($m_{\tilde{t}_1} > m_{\tilde{\chi}_1^0}$). As we will see shortly, in this scenario, the A_t parameter most likely gives rise to the largest fine-tuning, even when μ parameter is relatively large, i.e. about 700 GeV.

Concerning the bounds from direct SUSY searches at the LHC, let us take the gluino as an example. Gluino is the most copiously produced sparticle because of its strong coupling and high color multiplicity. However, searches for direct gluino pair production accompanied by $\tilde{g} \rightarrow q\bar{q}\tilde{\chi}$ decay [33, 34] show that if the LSP mass is greater than ~ 500 GeV, any gluino heavier than this mass can be safely undetected. In order to have the bound $m_{\tilde{g}} \gtrsim 1100$ GeV, only $m_{LSP} \gtrsim 400$ GeV is required because of the smaller production rate. These bounds become a little bit strong for $\tilde{g} \rightarrow t\bar{t}\tilde{\chi}$ and $\tilde{g} \rightarrow b\bar{b}\tilde{\chi}$ which are the favoured decay chains in natural SUSY. The corresponding limit for the LSP mass becomes a little higher because these searches use b-tag as signal discriminator and then does not depend on the energy of final states so much. The gluino can evade all the LHC searches for $m_{LSP} \gtrsim 700$ GeV. And the LSP mass drops to ~ 600 GeV for gluino with mass larger than ~ 1100 GeV [6, 35–40]. The corresponding bounds can be relaxed in the realistic MSSM since there will be suppression from branching fractions. Moreover, the existence of intermediate on-shell stop or sbottom tends to loose the bounds as well if the stop mass is either close to the gluino mass or the LSP mass. Similar results hold for the first two-generation squarks, stops and sbottoms, sleptons, charginos, and neutralinos, respectively.

Based on the fact that all the decay products of sparticles can be soften dramatically when the LSP mass is lifted, we propose the heavy LSP SUSY, which can evade the current

LHC SUSY search constraints while maintain the naturalness condition. To understand why all the current LHC SUSY search constraints can be escaped, we define an energy scale measure P to estimate the typical energy of a process, and present the detailed kinematic analyses both analytically and numerically. Also, using the distributions of the collider observables that are related to P , we can derive the shape of cut efficiency approximately for an experimental analysis. In particular, all the current LHC SUSY search constraints can be evaded if the LSP mass is around 600 GeV or higher. In the MSSM, we find that the heavy LSP SUSY does not generate more fine-tuning than Higgs boson mass. Based on all the current LHC SUSY searches, we systematically study the viable parameter space for heavy LSP SUSY, and present four benchmark points which realize our proposal concretely. What is more, a ~ 600 GeV wino LSP can generate the $(g - 2)_\mu$ excess as well [41].

This paper is organized as follows. In Section 2, we will discuss the effects of the LSP mass on the energy scale of the final states in details. In Section 3, based on the Barbieri-Giudice measure, we study the sources of fine-tuning in heavy LSP SUSY. We survey the realistic heavy LSP scenario in the MSSM in Section 4. In Section 5, after considering the constraints from the LHC direct searches, we systematically study the viable parameter space with heavy LSP SUSY in the MSSM and propose four benchmark points. Finally, some discussions and conclusions are given in section 6.

2 Kinematic Analysis of HLSP SUSY

2.1 Kinematic Analysis

As one can see in the exclusion plots provided by the ATLAS and CMS Collaborations [6, 33–40], no bounds can be drawn for the masses of mother sparticles such as gluino, stop, sbottom, squarks, electroweakinos, and sleptons when the LSP goes heavy as $500 \sim 600$ GeV, because of the softness of decay products and small missing energy. Because natural SUSY requires light gluino and stops, the heavy LSP SUSY could fit this requirement very well, and escapes from the LHC SUSY search constraints simultaneously.

To satisfy the natural SUSY requirement and accommodate large enough muon anomalous magnetic moment, we can define the Heavy LSP (HLSP) SUSY as follows: gluino is around $\gtrsim 1$ TeV, stop is lighter than 800 GeV, the electroweakinos and sleptons are as light as possible, and the LSP is as heavy as 500 – 600 GeV or even heavier. In fact, the HLSP SUSY can be regarded as a hybrid of the natural SUSY and compressed SUSY. In this Section, we will explain how the concept of the HLSP SUSY works in the collider aspect, via both analytical and numerical studies.

Let us start with the simplest case: a sparticle with mass M decaying into one massless SM particle and one LSP with mass m . In the rest frame of mother particle, we have the momentum magnitude of two daughter particles as they have the same momentum from momentum conservation

$$P = \frac{M^2 - m^2}{2M} = \frac{M}{2} \left(1 - \frac{m^2}{M^2}\right), \quad (4)$$

which is related to the LSP mass m quadratically. When $r = m/M$ goes up to $1/2$, P will

drop to $\frac{M}{2} \times \frac{3}{4}$ – a shift in 25%. This P is the most important measure in our HLSP SUSY which determines the whole energy scale of the decay process, as one will see clearly in the following analyses. Assuming uniform angular distribution, We therefore have the following average transverse energy for the visible SM decay product

$$p_T^{vis} = \langle p_T \rangle \sim \langle \sin \theta \rangle P \sim \frac{2}{\pi} P, \quad (5)$$

where θ is the angle between momentum and the beam pipe direction. The sparticles are mainly produced in the threshold region, so the boost effects can be safely ignored in a general analysis. Thus, we can have the collider observables expressed by the above momentum p_T^{vis} as a typical energy scale

$$E_T^{\text{miss}} \sim 2 \langle \cos \phi \rangle p_T^{vis} \sim \frac{4}{\pi} p_T^{vis}, \quad (6)$$

$$H_T \sim 2 p_T^{vis}, \quad (7)$$

where E_T^{miss} is transverse energy of the LSP, $H_T = \sum_{i=1}^{N_{\text{jet}}} p_T^i$ is the scalar sum of jet transverse momenta in the final state, and ϕ is half of the angle between the two genuine missing momenta. Therefore, all the observable energy scales are related to the typical energy scale P we defined previously. In the following analysis, we will use P as a main energy measure in collider analysis.

If we go from two-body to three-body decay, with the SM decay products massless, then we can work on it in a similar way as in two-body case. By combining the two visible massless particles into a massive one whose mass is the invariant mass the the original two, we obtain the visible energy

$$p_1^{vis} + p_2^{vis} = \frac{M^2 - m^2 + m_{12}^2}{2M}, \quad (8)$$

$$\sqrt{(p^{\text{miss}})^2 + m^2} = \frac{M^2 - m_{12}^2 + m^2}{2M}, \quad (9)$$

were p_1^{vis} and p_2^{vis} are the scalar momenta of the two SM particles, p^{miss} is the LSP moment, and $m_{12} = \sqrt{2p_1^{vis}p_2^{vis}(1 - \cos \theta)}$ is the invariant mass of system of two visible particles with θ the angle between the two momenta. When the two daughters goes in the same direction, then $m_{12} = 0$ and we come back to the massless two-body decay case. When they go back to back, we will get $m_{12, \text{max}}$. Also, we have $p^{\text{miss}} = \frac{\lambda^{1/2}(M^2, m_{12}^2, m_3^2)}{2M} < P$ with $\lambda(x, y, z) = x^2 + y^2 + z^2 - 2xy - 2xz - 2yz$. Because the total energy, which is determined by M , is barely changed, we have a shift in the observables, respect to the 2-body decaying case. Thus, we have a smaller transverse missing energy and a larger H_T for three body decay from Eqs. (8) and (9). The same reasoning can go further. If the SM product is a top quark which has a non-zero mass and then would decay, we call the topology as a multi-body decay. In this case, the missing energy would decrease further, but not change too much, respect to 3-body decay, as will be shown in the numerical analysis. Actually, from n -body to $(n + 1)$ -body: the more split one has, the softer each particle would be.

	(1000,0)	(1000,100)	(1000,200)	(1000,300)	(1000,400)	(1000,500)	(1000,600)	(1000,700)	(1000,800)
$\tilde{g} \rightarrow g\tilde{\chi}$ at LHC-8	554	550	534	508	480	435	385	335	282
$\tilde{g} \rightarrow q\bar{q}\tilde{\chi}$ at LHC-8	362	362	363	348	330	299	253	228	178
$\tilde{g} \rightarrow q\bar{q}\tilde{\chi}$ at LHC-13	373	378	374	365	341	307	268	244	204
$\tilde{g} \rightarrow t\bar{t}\tilde{\chi}$ at LHC-13	376	378	374	363	344	311	268		

Table 1: Expected values of E_T^{miss} for different LSP masses and different decay channels. The numbers in the first row give the gluino and LSP masses.

	(1000,0)	(1000,100)	(1000,200)	(1000,300)	(1000,400)	(1000,500)	(1000,600)	(1000,700)	(1000,800)
$\tilde{g} \rightarrow g\tilde{\chi}$ at LHC-8	1074	1066	1045	996	936	851	752	645	534
$\tilde{g} \rightarrow q\bar{q}\tilde{\chi}$ at LHC-8	1267	1231	1158	1072	961	850	716	598	444
$\tilde{g} \rightarrow q\bar{q}\tilde{\chi}$ at LHC-13	1391	1356	1263	1175	1070	945	809	681	523
$\tilde{g} \rightarrow t\bar{t}\tilde{\chi}$ at LHC-13	1381	1348	1271	1168	1066	952	813		

Table 2: Expected values of H_T for different LSP masses and different decay channels. The numbers in the first row give the gluino and LSP masses.

However, this shift is small in most cases. It should be noticed that only the final state jets with transverse energy above some thresholds are considered at the hadron collider, which makes our above discussion as an approximation. As we will see later, the H_T of three body decay is indeed smaller than H_T of two body decay in the relatively compressed region. This is mainly because in this region, there is great possibility that the softer jets of three body decay go below the energy threshold ($p_T < p_{T_{\text{min}}}$) or go outside the detector ($|\eta| > \eta_{\text{max}}$).

Now we have seen that the energy observables such as E_T^{miss} and H_T depend on the energy measure P we defined previously. As for P , for a fixed M , it depends on the LSP mass quadratically. The heavy LSP would play an important role in such cases: when mother particle is light as several hundred GeV, the energy scale P is around several hundred GeV and thus the cut efficiency would be very sensitive to the shift of P ; or when mother particle is heavy enough (thus has a rather small production cross section) to be sensitive to minor shift of cut energy (thus the shift of cut efficiency).

2.2 Numerical Study of the Heavy LSP Effects

To put it more realistic, we consider three typical decay chains for gluino as an illustration: 1) $\tilde{g} \rightarrow g\tilde{\chi}$; 2) $\tilde{g} \rightarrow q\bar{q}\tilde{\chi}$; 3) $\tilde{g} \rightarrow t\bar{t}\tilde{\chi}$. We use MadGraph5 [42] to generate the $\tilde{g}\tilde{g}$ pair production with subsequent decays. Pythia6 [43] is used for parton showering and hadronization. And we use PGS4 [44] for detector simulation. To calculate the LSP mass dependence, we fix $m_{\tilde{g}} = 1000$ GeV. And to estimate the overall behaviour of each model, we average over 50,000 events for each variable. The averaged $E_T^{\text{miss}}(\langle E_T^{\text{miss}} \rangle)$ and $H_T(\langle H_T \rangle)$ for different LSP masses and different decay channels are given in Tables 1 and 2, respectively.

Therefore, our conclusions from the numerical results are

- The P measure works very well for all decay channels. Both $\langle E_T^{\text{miss}} \rangle$ and $\langle H_T \rangle$ are proportional to the corresponding P of each channel and decrease quadratically with increasing LSP mass.

- The ratio of $\langle E_T^{\text{miss}} \rangle$ and $\langle H_T \rangle$ for two-body decay are indeed approximated by Eqs. (6) and (7), especially at the large mass splitting region.
- As we have noted before, H_T will deviate a little from theoretical prediction for three body decay due to the detector effects. In Table 2, the $\langle H_T \rangle$ of three-body decay decreases much faster than two-body decay when the LSP mass increases, and becomes smaller than the two-body decay around $m = \frac{M}{2}$ for different collision energies and different decay channels.
- There are considerable shifts for energy observables from two-body to three-body decays from Table 1. This point would have an impact on the collider searches for gluino, since the missing energy cut would lose some efficiencies because of the shift downwards.
- From three-body to multi-body, there is no significant change for both $\langle E_T^{\text{miss}} \rangle$ and $\langle H_T \rangle$.
- From 8TeV to 13/14 TeV LHC, both $\langle E_T^{\text{miss}} \rangle$ and $\langle H_T \rangle$ get an increase because of the increasing hardness of the final states, as expected for the larger Center Mass (CM) energy. However, the increasing is only mild.

In addition, we employ very naive E_T^{miss} and H_T cuts to visualise how the cut efficiency is reacting respect to the LSP mass variance. We plot the cut-efficiencies for two-body decay at 8 TeV LHC, three body decay at 8 TeV LHC, three body decay at 13 TeV LHC, and multi-body decay at 13 TeV LHC with $M = 1$ TeV in Fig. 1.

The P , which measures the overall hardness of a process, is decreased quadratically with the LSP mass. Thus, the cut efficiency drops much faster when m goes heavier for all cases. From Fig. 1, we can also conclude that when $r = m/M$ becomes relatively large such that $P \sim E_{\text{cut}}$, it experiences a big drop. Moreover, for harder cuts, the LSP mass would play an more important role for cut efficiency. As one can see, the multi-body decay case does not differ from the three-body decay case, and the 13 TeV results are almost the same as the 8 TeV ones, which makes sense since the cut energy we employ are relatively low thus the cut efficiencies remain the same for higher collider energy.

Having checked more benchmark points, we are led to an empirical formulae for the cut efficiencies where the E_T^{miss} and H_T distributions have a general pattern

E_T^{miss} cut	$\langle E_T^{\text{miss}} \rangle / 2$	$\langle E_T^{\text{miss}} \rangle$	$2\langle E_T^{\text{miss}} \rangle$
$\epsilon \sim$	0.83	0.5	0.03-0.05
H_T cut	$2/3\langle H_T \rangle$	$\langle H_T \rangle$	$5/3\langle H_T \rangle$
$\epsilon \sim$	0.82	0.45	0.05

Table 3: The cut efficiencies for different cuts which are scaled by the specific energy scale. We are presenting the empirical results here.

The distribution of missing energy is expected to be approximated by a normal distribution with a central value at $\langle E_T^{\text{miss}} \rangle$, and $\sigma \sim \langle E_T^{\text{miss}} \rangle / 2$, while H_T has a central value of $\langle H_T \rangle$

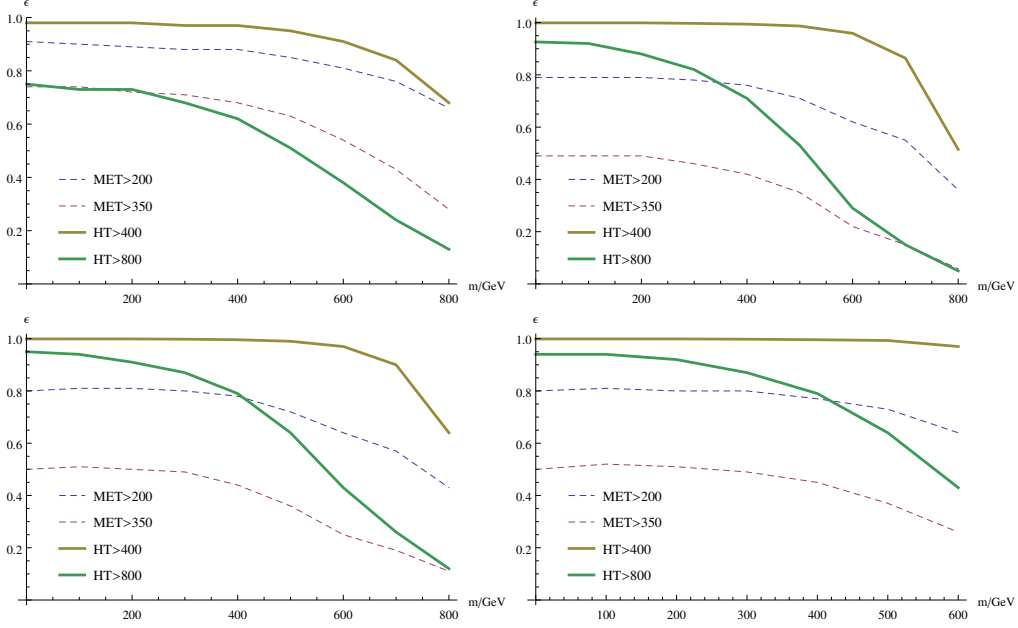


Figure 1: The cut efficiencies for naive cuts displayed for four cases with $M = 1$ TeV. From left to right, top to bottom, we display two-body decay at 8 TeV LHC, three-body decay at 8 TeV LHC, three-body decay at 13 TeV LHC, and multi-body decay at 13 TeV LHC, respectively.

and $\sigma \sim \langle H_T \rangle / 3$. With this approximation, we can analytically “guess” the cut efficiencies for any benchmark points. In Fig. 2, we show the cut efficiencies for missing energy cuts of 200 GeV and 350 GeV, using the Gaussian approximation for the distributions of E_T^{miss} . It highly agrees with the realistic one in Fig. 1 with $P \sim \Delta m = M - m$. These is a region the cut efficiency drops very fast, which corresponds to our HLSP scenario. In this region ($E_{\text{cut}}/2 \sim 2E_{\text{cut}}$), the cut efficiencies change violently with the m variance.

Therefore, in the sense of kinematic analysis, we can redefine the heavy LSP SUSY as follows: the LSP mass is large enough to give an impact on the general energy cuts (a visible amount (e.g. a half) of the cut efficiency drop respect to the massless LSP case). For a typical mother particle mass $M \sim 1$ TeV (which is the typical value of gluino mass in natural SUSY), the mass m , which gives a typical cut efficiency of 0.5, makes the LSP heavy. For such a heavy LSP, stops and sbottoms are always safe. Thus, at the first sight, the HLSP seems a cut-dependent concept. However, with collider energy given, the cut energy scale does not vary too much since the background is well understood.

2.3 Cuts Efficiency Versus Cross Section

With the above kinematic analysis, we can make the realistic collider analysis. The typical search strategies at the ATLAS and CMS experiments are applying some cuts on characteristic kinematic variables such as missing transverse energy or the total hadronic energy of one single event. Besides these simple cuts, sometimes other advanced techniques such as

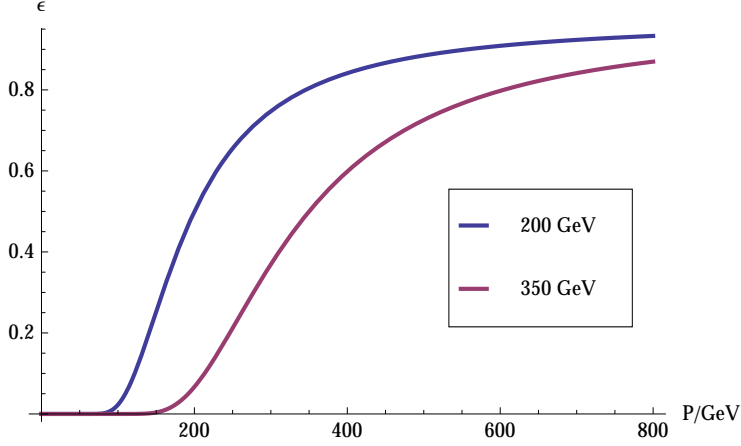


Figure 2: Analytic plot of the cut efficiencies for cut energies 200 and 350 GeV. We are using Gaussian distribution for simulation.

b-tagging or jet-substructure are employed. Although the LSP mass would play a role in these advanced techniques, the most important changes would go to the energy cuts. So it is important to work in the toy models where just energy cuts are considered. In our work, only these basic selections are taken into investigation.

In collider searches, there are two competing factors: one is the production cross section, and the other is the cut efficiency (Strictly speaking, it is cut-efficiency (ϵ) multiplied by acceptance (A)). In general, the cross section decreases exponentially as the sparticle mass increases. Because the sparticle pairs are mainly produced at their mass thresholds, the partonic cross-sections fall as $1/\hat{s} \sim 1/(4M^2)$, where $\sqrt{\hat{s}}$ represents the CM energy of the parton system. At the hadronic level, we have

$$x_1 x_2 S = \hat{s} \sim 4M^2, \quad (10)$$

where x_1 and x_2 represent the parton momentum fractions, and S represents the hadronic squared CM energy. Taking $\sqrt{s} = 8$ TeV for the LHC8 and sparticle mass $M \sim 1$ TeV, we get $x_1 x_2 \sim 1/16$. So the typical values for x lie in the large- x regime. Note that the LHC is a proton-proton collider, most SUSY events are generated through gluon fusion. So the gluon PDF plays an important role here. In the large- x region, PDF decreases exponentially. Thus, the production cross section also decreases exponentially, respect to the increasing of sparticle mass.

As for the cut efficiency, the lucky fact is that for a given LSP mass, the heavier the mother particle is, the more energetic the products are, and then the higher the cut efficiency is. Thus, in most cases, we would have cut efficiency scaled as the mass splitting of mother and daughter particles $\Delta m = M - m$. The contour of cut-efficiency is

$$\frac{M}{2} \left(1 - \frac{m^2}{M^2}\right) = P, \quad (11)$$

$$M = P + \sqrt{P^2 + m^2}. \quad (12)$$

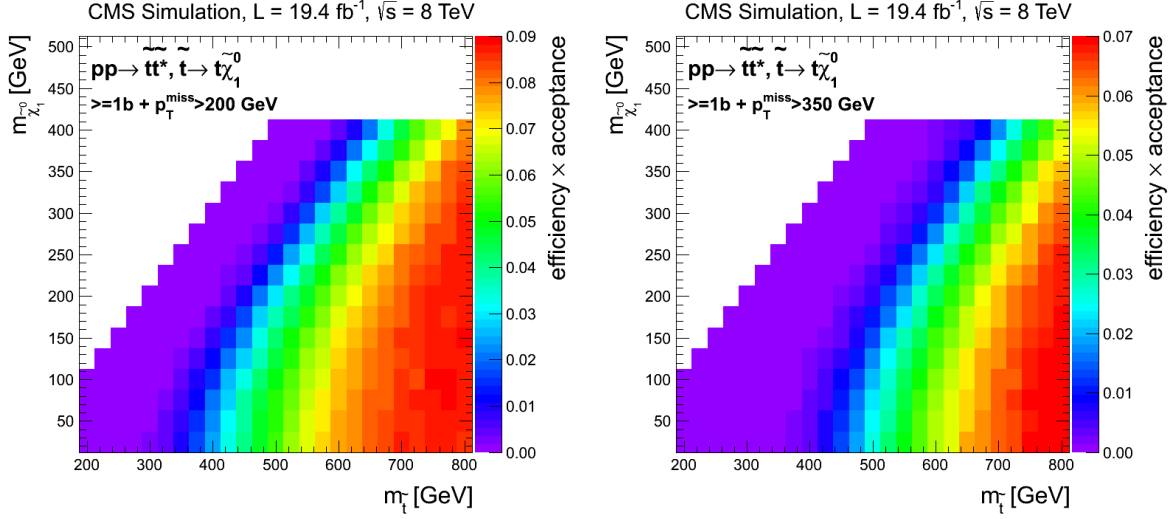


Figure 3: The cut efficiencies from the CMS experiment [45].

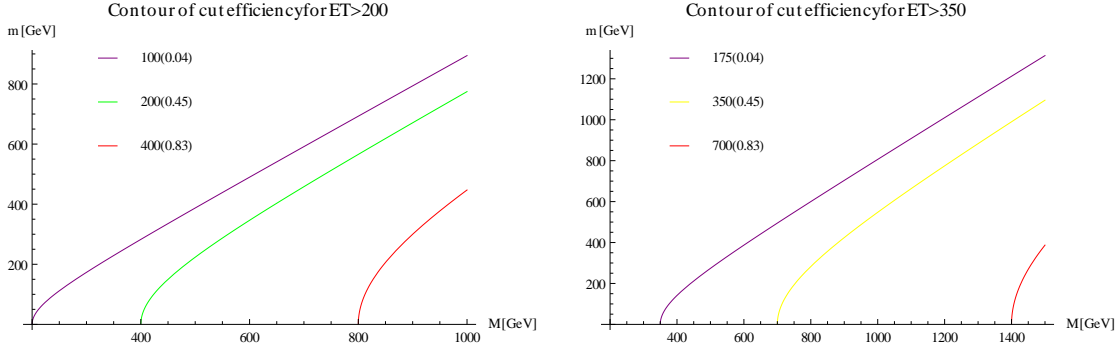


Figure 4: Contours of the cut efficiencies for a specific cut. We show both the energy measure and cut-efficiency, where the cut efficiency is put in the bracket.

For the same P , one gets the same cut efficiency for a specific cut such as $E_T^{\text{miss}} > 200$ GeV. When m goes significantly larger than P , we approximately have $M \simeq P + m + \frac{P^2}{2m} = (1 + \frac{P}{2m})P + m$, thus $P \sim \Delta m = M - m$. This is the reason why only Δm matters in that region.

For the sake of illustration, we take two cut efficiency plots from the CMS Collaboration [45] as examples. In Fig. 3, the cut efficiency \times acceptance is shown for the simplified model $pp \rightarrow t\bar{t}^*$, and $\tilde{t} \rightarrow t\tilde{\chi}_1^0$. Also, the left one is for selection ($\geq 1b + E_T^{\text{miss}} > 200$ GeV), while the right one is for the selection ($\geq 1b + E_T^{\text{miss}} > 350$ GeV). One can see that for a fixed M , as m_{LSP} becomes heavier, the cut efficiency drops faster and faster. When the mass scales goes higher for both sparticles, the contours become lines, which mean only Δm matters here. When the larger energy cut is imposed, the cut efficiency drops, and the whole contour would shift. We work in the two-body decay simplified model, and produce

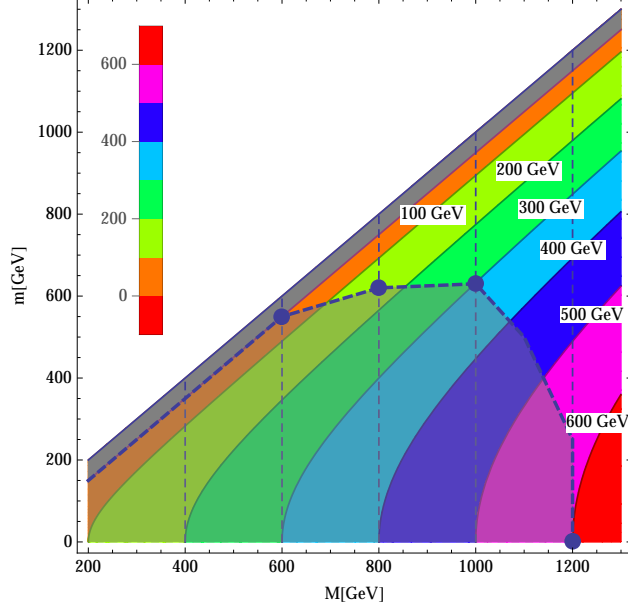


Figure 5: The contours of energy measure P in the simplified model for two-body decay with mother sparticle mass M , and the LSP mass m . The compressed region is shaded with grey, while the excluded region is shaded with light grey.

the contour for naive cuts $E_T^{\text{miss}} > 200/350$ GeV in Fig. 4. The shapes fit with the realistic ones very well, which strongly suggests that the P measure and the empirical formulae for cut efficiency indeed work here.

2.4 Reproducing the Experimental Exclusion Bounds Conceptually

Up to now we already have all the relevant elements established which are needed to achieve the experimental exclusion bounds and the core idea of the HLSP SUSY.

In order to illuminate how the HLSP SUSY works, we reproduce the SUSY exclusion plot in concept. We consider the two-body decay simplified model for simplicity and transparency, where the mother sparticle has mass M , the visible SM products are massless, and the LSP has mass m . In Fig. 5, we at first present the contours of the typical energy scale (P) (with step of 100 GeV). These contours of energy scale can be easily translated to those of cut efficiency for a specific cut on missing energy or total visible energy of a single event, according to the empirical formulae we discussed in the previous subsection. At the 7 & 8 TeV LHC, the typical missing energy cuts lie in the range of $50 \sim 350$ GeV. As for a 200 GeV cut of missing energy, the line starting from $(M = 400 \text{ GeV}, m = 0 \text{ GeV})$ thus has $P \sim 200$ GeV and would assemble those points with cut efficiency $\epsilon \sim 0.5$. One can see that the closer the benchmark point is to the kinematic border, the faster the ϵ drops (the sudden drops in Fig. 2). It drops exponentially when the model point is close to the border, which is reigned by the “compresses SUSY” scenario. Further to the border, when increasing the

Δm from the energy of cut and going to the massless LSP region, the ϵ experiences a flat and slow growing, until reaching the maximum ϵ_{max} . This is the region for the “classical” SUSY scenario, where the LSP mass can be safely ignored in collider search.

We shadow the compressed region ($\Delta m \sim 50$ GeV) in grey, and the typical LHC exclusion bounds (generically massless to medium LSP) in light grey. As for the energy of cut which is designed depending on the collider energy and the investigated process, it can be estimated using the general sparticle masses which are in the search, i.e. $H_{Tcut} \sim M_{SUSY}$. At the current stage, we only discuss about the LHC-8 and the forthcoming LHC-13/14. In addition, as we have seen in the last subsection, multi-body decay would not change the physics picture too much respect to two-body decay of the mother particles.

As the number of events for a specific signal region is expressed as $N_{SUSY} = \epsilon \times A \times \sigma_{SUSY} \times \text{Luminosity}$, the cut efficiency (ϵ) and the production cross section (σ_{SUSY}) compete for a given upper limit of event numbers (say, for 95% exclusion). Because the σ_{SUSY} drops exponentially according to the mass M , the contours of cross sections are lined vertically, as indicated by dashed lines in Fig. 5. Assuming a constant ϵ in the whole parameter space, we would get a vertical exclusion bound, which indicates a lower limit of M no matter how heavy m is. However, the $\epsilon \times A$ are not vertically scaled. They are generally scaled with $\Delta m = M - m$. When m gets larger (till $\Delta m \sim E_{cut}$), the cut efficiency drops very fast and then bends the exclusion curve towards small M region, which has a larger production cross section, as shown in Fig. 5. Finally, it ends in the compressed regime with a much smaller M respect to massless LSP case. Remember that ϵ drops exponentially near the compressed regime, this drop in the cut efficiency plays the major role in the HLSP SUSY. The point is that the “inefficiency” helps natural SUSY with a heavy enough LSP to escape the LHC search constraints.

Until now, we have presented the main idea of heavy LSP SUSY. As a summary, we list four important conclusions of this section

- The typical energy measure P determines the most general characteristics of an event, such as $E_T^{miss} \sim P$ and $H_T \sim 2P$.
- The cut efficiency generally lines with Δm when m is much larger than P , and drops much faster along the heavier LSP mass, especially in the region $\sim [P/2, 2P]$.
- The horizontal shape of the exclusion curve at $600 \text{ GeV} \lesssim M \lesssim 1000 \text{ GeV}$ in Fig 5 is due to the cancellation between the exponential increase of cut efficiency and the exponential decrease of production cross section with increasing M .
- The HLSP proposal is very important in these specific cases: 1) A heavy enough LSP (close to the compressed region); 2) A medium to heavy LSP when the production cross section is very small (M is large enough).

Therefore, we come up with two HLSP SUSY definitions: one from the collider/kinematic aspects while the other from the SUSY phenomenology. The “collider” definition is $\frac{m}{M} \gtrsim \frac{1}{2}$; while the definition for SUSY phenomenology is more relaxed: $200 \lesssim \Delta m \lesssim 600 \text{ GeV}$ where a little bit lighter spectra would help to explain the anomalous magnetic moment of muon, which have taken into account the scale of natural SUSY and current LHC SUSY bounds.

3 Fine-Tuning of the MSSM with Heavy LSP

In previous Sections, we have studied the HLSP SUSY from the kinematic point of view. Next, we shall discuss the naturalness of a specific supersymmetric model, the MSSM, in which a heavy LSP is imposed.

In the MSSM, the naturalness problem arises from the tadpole equation which determines the Z boson mass m_Z

$$\frac{m_Z^2}{2} \simeq \frac{m_{H_d}^2 - \tan^2 \beta m_{H_u}^2}{\tan^2 \beta - 1} - \mu^2, \quad (13)$$

where all the parameters are defined at electroweak (EW) scale. The following quantity was proposed [46, 47] to measure the degree of fine-tuning of the above equation

$$\Delta_Z = \max_i F_i, \quad F_i = \left| \frac{\partial \ln m_Z}{\partial \ln p_i} \right|, \quad (14)$$

with p_i are the fundamental parameters at the fundamental scale, for instance, the unification scale in the Grand Unified Theory (GUT).

Because our fundamental theory is usually defined far above the EW scale, we need to express the Higgs soft masses m_{H_u} , m_{H_d} and μ in Eq. 13 in terms of fundamental parameters before calculating the degree of fine-tuning in Eq. 14. Previous studies [48, 49] have shown that the soft parameters at low energy scale are polynomial functions of the corresponding parameters at fundamental scale, whose coefficients depend on the Yukawa couplings and gauge couplings. To derive the polynomial functions by solving the Renormalization Group Equations (RGEs), we consider the following MSSM soft terms

$$\begin{aligned} -\mathcal{L}_{\text{soft}}^{\text{MSSM}} = & -\frac{1}{2}(M_3 \tilde{g}\tilde{g} + M_2 \tilde{W}\tilde{W} + M_1 \tilde{B}\tilde{B} + h.c.) \\ & + [-a_t H_u \tilde{Q}\tilde{t} + a_b H_d \tilde{Q}\tilde{b} + a_\tau H_d \tilde{L}\tilde{\tau} + h.c.] + (\text{first two generation}) \\ & + [\bar{m}_Q^2 \tilde{Q}^* \tilde{Q} + \bar{m}_L^2 \tilde{L}^* \tilde{L} + \bar{m}_t^2 \tilde{t}^* \tilde{t} + \bar{m}_b^2 \tilde{b}^* \tilde{b} + \bar{m}_\tau^2 \tilde{\tau}^* \tilde{\tau}] + (\text{first two generation}) \\ & + [m_{H_u}^2 H_u^* H_u + m_{H_d}^2 H_d^* H_d + (b H_u H_d + h.c.)]. \end{aligned} \quad (15)$$

As a convension, we have defined the following parameter:

$$a_t = y_t \bar{A}_t, \quad a_b = y_b \bar{A}_b, \quad a_\tau = y_\tau \bar{A}_\tau, \quad (16)$$

where the y_i are corresponding Yukawa couplings.

For example, in the MSSM with $\tan \beta = 20$ [50–52], if we choose the fundamental scale to be the GUT scale $\sim 2 \times 10^{16}$ GeV, without take into account any threshold effects, we can express the EW scale $m_{H_u}^2$ and $m_{H_d}^2$ as follows

$$\begin{aligned} m_{H_u}^2 \simeq & -2.82 \bar{M}_3^2 + 0.206 \bar{A}_b^2 - 0.15 \bar{A}_b \bar{M}_3 - 0.23 \bar{A}_t^2 + 0.48 \bar{A}_t \bar{M}_3 \\ & - 0.026 \bar{m}_b^2 - 0.42 \bar{m}_Q^2 - 0.33 \bar{m}_t^2 + 0.57 \bar{m}_{H_u}^2 + \dots, \end{aligned} \quad (17)$$

$$\begin{aligned} m_{H_d}^2 \simeq & -0.83 \bar{M}_3^2 - 2.6 \bar{A}_b^2 + 1.48 \bar{A}_b \bar{M}_3 + 0.06 \bar{A}_t \bar{M}_3 \\ & - 0.07 \bar{m}_b^2 - 0.06 \bar{m}_Q^2 - 0.06 \bar{m}_t^2 + 0.85 \bar{m}_{H_d}^2 + \dots, \end{aligned} \quad (18)$$

where the parameters with bar are defined at the GUT scale and the dots denote ignorable terms, and we have used the SM parameters as below

$$\begin{aligned} m_t &= 173.4 \text{ GeV}, \quad m_b = 4.25 \text{ GeV}, \quad m_\tau = 1.777 \text{ GeV} \\ \alpha_1 &= 1/58.97, \quad \alpha_2 = 1/29.6, \quad \alpha_3 = 1/8.4. \end{aligned} \quad (19)$$

At the large $\tan \beta$ limit, Eq. (13) can be rewritten as

$$m_Z^2 \simeq -2m_{H_u}^2 - 2\mu^2. \quad (20)$$

After substituting $m_{H_u}^2$ in Eq. (17), we obtain

$$\begin{aligned} m_Z^2 &\simeq -2\mu^2 + 5.64\bar{M}_3^2 - 0.412\bar{A}_b^2 + 0.3\bar{A}_b\bar{M}_3 + 0.46\bar{A}_t^2 - 0.96\bar{A}_t\bar{M}_3 \\ &\quad + 0.052\bar{m}_b^2 + 0.84\bar{m}_Q^2 + 0.66\bar{m}_t^2 - 1.14\bar{m}_{H_u}^2 + \dots, \end{aligned} \quad (21)$$

where the small radiative corrections of μ have been neglected. This is the ultimate equation that we will use to estimate the degree of fine-tuning in the MSSM. In light of Eq. (14), we then calculate the corresponding degree of fine-tuning for each parameter

$$\begin{aligned} F_\mu &\simeq 2 \times \frac{\mu^2}{m_Z^2}, \quad F_{\bar{M}_3} \simeq (2 \cdot 5.64\bar{M}_3 - 0.96\bar{A}_t) \times \frac{\bar{M}_3}{2m_Z^2}, \\ F_{\bar{m}_Q} &\simeq 0.84 \times \frac{\bar{m}_Q^2}{m_Z^2}, \quad F_{\bar{m}_t} \simeq 0.66 \times \frac{\bar{m}_t^2}{m_Z^2}, \\ F_{\bar{A}_t} &\simeq (2 \cdot 0.46\bar{A}_t - 0.96\bar{M}_3) \times \frac{\bar{A}_t}{2m_Z^2}. \end{aligned} \quad (22)$$

In our heavy LSP SUSY, the LSP is usually required to be above ~ 600 GeV so that the current LHC SUSY search constraints can be evaded. In order to have all higgsinos heavier than this mass scale, μ should be $\gtrsim 600$ GeV. This will give us the least degree of fine-tuning in the HLSP SUSY, which is

$$F_\mu \simeq 87 \sim \mathcal{O}(100). \quad (23)$$

In the following discussions, this value will be regarded as a reference degree of fine-tuning for natural MSSM with heavy LSP. And then

$$\bar{M}_3 \lesssim 380 \text{ GeV} \quad (24)$$

is required if there is no more fine-tuning produced by gluino. And the EW-scale gluino mass can be estimated by $m_{\tilde{g}} \lesssim 2.9\bar{M}_3 \simeq 1.1$ TeV. On the other hand, because of the gluino large production rate, its mass has been excluded up to 1.4 TeV and 1.3 TeV [6, 35–40] when it is decaying into $t\bar{t}\tilde{\chi}$ and $b\bar{b}\tilde{\chi}$, respectively. Even if gluino decays into the first two-generation squarks, where the flavour-tag no longer works, the exclusion bounds can be still as high as 1.4 TeV [33, 34]. To save a light gluino with mass around 1.1 TeV, in turn we need the heavy

LSP to soften the final states as discussed in Section 2. This is the reason why the heavy LSP SUSY servers as the simplest and most reliable scenario for natural MSSM.

Similarly, by requiring no more than $\sim \mathcal{O}(100)$ degree of fine-tuning in stop sector, we get

$$\bar{m}_{Q_3} \lesssim 990 \text{ GeV}, \quad \bar{m}_t \lesssim 1120 \text{ GeV}, \quad \bar{A}_t \lesssim 1400 \text{ GeV} . \quad (25)$$

Note that these values just satisfy the requirements of implementing ~ 125 GeV Higgs boson mass in the MSSM. As a result, the stop sector remains the main source of fine-tuning while the LSP mass can naturally be heavy in the heavy LSP MSSM.

4 Surveying the Heavy LSP MSSM

4.1 The Parameter Space

The MSSM is the most well studied SUSY model, not only because it is simple but also it can explain many new phenomena beyond the SM. The muon anomalous magnetic moment $a_\mu = (g - 2)/2$ is one of most precisely measured value, which shows more than 3σ -level discrepancy from the SM. The extra contributions from neutralinos/charginos and sleptons in the MSSM might provide a solution to the $(g - 2)_\mu$ problem. We require the MSSM to have the a_μ within the 3σ of its theoretical prediction [53–56]

$$4.7 \times 10^{-10} \leq a_\mu \leq 52.7 \times 10^{-10} \quad (26)$$

when we scan the parameter space. The SM-like Higgs boson in the MSSM should have mass around 125 GeV as well. Considering both the uncertainties from experiments and theoretical calculations, we impose

$$123.5 \text{ GeV} \leq m_h \leq 127.5 \text{ GeV} . \quad (27)$$

The signal strength of the Higgs boson for all decaying channels are assured to be highly SM-like if we are working in decoupling region which is always true in our following discussions. The first discovery of branching fraction of $B_s \rightarrow \mu^+ \mu^-$ at the LHCb [57], which is very close to the SM prediction, imposes a strong bound on new physics (95% CL)

$$2 \times 10^{-9} < \text{Br}(B_s \rightarrow \mu^+ \mu^-) < 4.7 \times 10^{-9} . \quad (28)$$

In the MSSM, the rate of the process is proportional to $\tan^3 \beta$. Because of the relatively large $\tan \beta$ we are considering about, Eq. (28) does give strong bound on our scenario essentially. In contrast, we find the branching fraction of $b \rightarrow s \gamma$ is always below the measured value after we have imposed the constraint from $(g - 2)_\mu$. So, we only suppose an additional flavour-violating soft term may compensate the value to fit with measurements and will not consider this experiment in the following discussions. Also, we will consider the constraints from dark matter relic density and dark matter direct detection in the next subsection.

We work at the GUT scale without implying any unification condition. Suspect2 [58] is used to calculate the mass spectra. And all the above mentioned experimental values are calculated by micromegas 3.2 [59, 60]. The parameters are scanned in the following ranges before we apply any optimisations

$$\begin{aligned}
& \tan \beta : [15, 40], \quad \mu : [500, 1000] \text{ GeV}, \quad M_A : [200, 2500] \text{ GeV}, \\
& \bar{M}_1 : [1200, 2500] \text{ GeV}, \quad \bar{M}_2 : [600, 1200] \text{ GeV}, \quad \bar{M}_3 : [330, 600] \text{ GeV}, \\
& \bar{A}_t : [-2300, 2300] \text{ GeV}, \quad \bar{m}_{L_{2,3}} : [400, 1000] \text{ GeV}, \quad \bar{m}_{e_{2,3}} : [400, 1000] \text{ GeV}, \\
& \bar{m}_{Q_3} : [200, 1400] \text{ GeV}, \quad \bar{m}_{U_3} : [200, 1700] \text{ GeV}, \quad \bar{m}_{D_3} : [100, 1900] \text{ GeV}, \\
& \bar{A}_b : [-2000, 2000] \text{ GeV}, \quad \bar{A}_l = 0 \text{ GeV}, \quad \bar{m}_{Q_2, U_2, D_2} : [1500, 3000] \text{ GeV}.
\end{aligned} \tag{29}$$

In order to find out the effects of naturalness on the HLSP SUSY, we have chosen the region which slightly wider than the natural SUSY region that we have discussed in Section 3. The gaugino mass ranges at the GUT scale are chosen such that at the EW scale bino and wino are within the mass range of $\sim [500, 1000]$ GeV while the mass of gluino is around $[900, 2000]$ GeV. Moreover, μ should be larger than 500 GeV to get a heavy LSP and smaller than 1 TeV as required by naturalness.

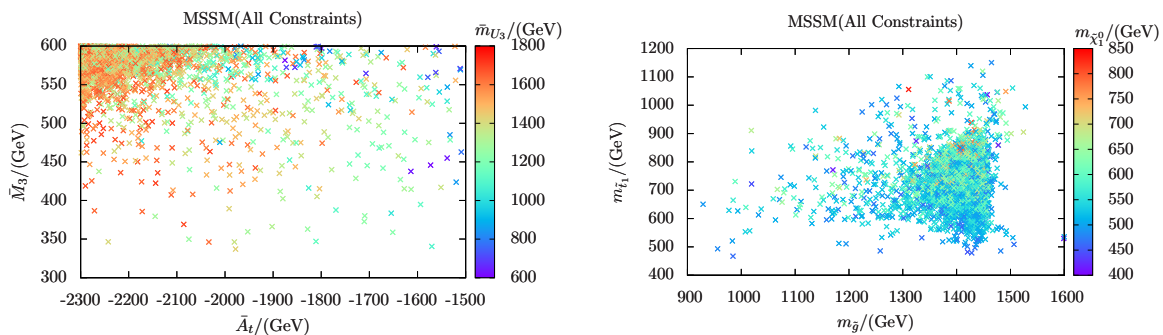


Figure 6: The viable parameter space in the heavy LSP MSSM which satisfies all the current constraints mentioned in the text except the dark matter constraints. Left: \bar{M}_3 versus \bar{A}_t with varying \bar{m}_{U_3} , which give the largest contribution to the fine-tuning measure. Right: the gluino mass versus the light stop mass with varying LSP mass.

To find out the tension between Higgs boson mass and naturalness in heavy LSP SUSY, we show the viable parameter space in the left panel of Fig. 6. Due to the heavy Higgs boson mass we have imposed, the upper-left region is highly favoured. However, the most natural region is at the lower-right of the $\bar{A}_t - \bar{M}_3$ plane, even though only a small parameter space survives in this region. Comparing the figure with Eqs. (24) and (25), we conclude that one of the equations has to be violated in order to get the properly large Higgs boson mass. Thus, the heavy LSP SUSY brings no more fine-tuning than the Higgs boson mass. In other words, in the HLSP SUSY, the dominant source of fine-tuning is still from Higgs boson mass. As for the stop soft masses, a relatively large mass splitting between two stop

mass eigenstates is preferred to implement the maximal-mixing in stop sector, and we find it is the \bar{m}_{U_3} preferred to be the larger one. So we vary it in the figure as well.

Also, we show the $m_{\tilde{g}}$, $m_{\tilde{t}_1}$ and $m_{\tilde{\chi}_1^0}$ on the right panel of Fig 6. The gluino mass and light stop mass can be as light as ~ 950 GeV and ~ 450 GeV respectively. And the maximal mixing scenario also guarantees that $|\bar{A}_t|$ can remain small (~ 1700 GeV), while Higgs boson mass is relatively large. The LSP mass is relatively free as long as it is smaller than the light stop mass.

4.2 The LSP Properties and Dark Matter Direct Detection

The heavy LSP can be an interesting dark matter candidate, so we will study its properties and direct detection potential. Because light wino and higgsino are preferred to enhance the SUSY $(g-2)_\mu$ contribution [61], either wino or higgsino can be the LSP in our scenario. To maintain these possibilities, we only require that the LSP be one component of dark matter sector. So the LSP relic density might be smaller than the Planck measurement 0.1187 [62].

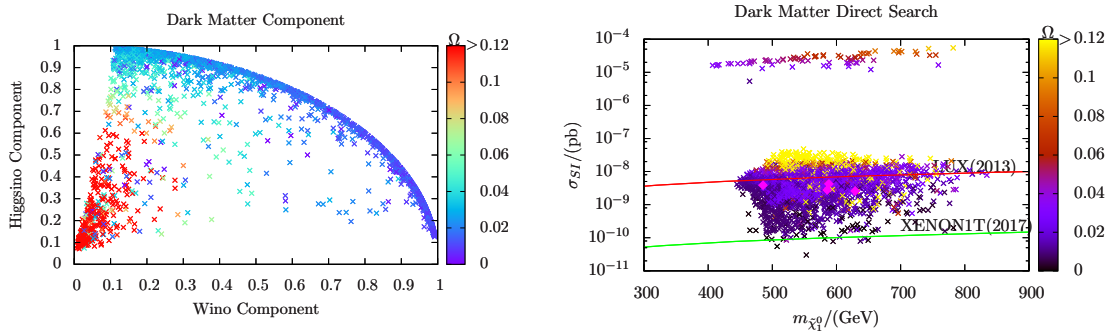


Figure 7: Left: The wino and higgsino components of the LSP neutralino. Right: the LSP mass versus the reduced spin independent proton-neutralino collision cross section. The color shows the dark matter relic density, where we have set those with $\Omega > 0.1187$ the same color.

In the left panel of Fig 7, we show the higgsino and wino components of the LSP neutralino. The color shows the relic density, and the red points with $\Omega > 0.1187$ are excluded. The major scanned parameter space has

$$\text{Wino component}^2 + \text{Higgsino component}^2 \sim 1. \quad (30)$$

Thus, the relic densities for those points are very small, e.g., about one order of magnitude smaller than the observed value. However, some points can still have small Ω while their bino component is large since the bino LSP can coannihilate with other sparticles, especially stop, to reduce the relic density.

We show the reduced spin independent dark matter direct detection rate in the right panel of Fig 7. The proton-neutralino collision cross section has rescaled by

$$\hat{\sigma}_{SI} = \frac{\Omega}{0.1187} \sigma_{SI} , \quad (31)$$

which we call it the reduced collision rate. The red and green lines show the bounds from the LUX experiment [63] and the expected XENON1T experiment [64], respectively. And the diamonds are those benchmark points which we will discuss later. The yellow points are excluded by over abundant dark matter. As we can see, a few of our viable points are already excluded by the LUX experiment and almost all the parameter space are within the reach of the XENON1T experiment. Most of the points with large wino and higgsino components satisfy the LUX experimental constraint because of the small relic density they have. And the others that have relatively large relic density can also keep undetected by the LUX experiment due to their large bino component.

The figure also shows a few points which have very large proton-LSP collision rate. For those points, the LSP is τ -sneutrino which has very large spin independent interaction with nucleon though Z boson exchange. Their relic density are mainly scaled by their masses, ranging from ~ 0.01 to ~ 0.1 with mass range $\sim [400, 800]$ GeV.

5 Confronting the LHC Data and Naturalness

The Higgs boson mass is not the only source of fine-tuning problem. Even after the realisation of a correct Higgs boson mass in the MSSM, either stop or gluino can be very light, as we have shown in Fig 6. However, there are also many direct SUSY searches at the LHC which push SUSY above the TeV scale. From discussions in Section 3, they might induce a much more serious fine-tuning problem. Unlike the constraint from Higgs boson mass, the direct SUSY searches increase the mass bounds on all sparticles simultaneously. In this Section, we will study the constraints from the LHC direct SUSY searches and find out how heavy the LSP can save the natural MSSM.

A light stop always exists in natural SUSY models. The searches for light stop are one of the main subjects on SUSY phenomenology. The ATLAS and CMS experimentalists have carried out many kinds of searches for direct stop production persistently. Stop can decay into $b\tilde{\chi}^\pm$ and $\tilde{\chi}^\pm \rightarrow W^{(*)}\tilde{\chi}$. Searches for final state with b-jets and leptons [65–67] have exclude the stop in this channel up to about 600 GeV. However, these searches are only sensitive when the LSP mass is smaller than ~ 300 GeV. The exclusion bound on stop mass can be higher if $\tilde{t} \rightarrow t\tilde{\chi}$, which is ~ 700 GeV when considering two hadronic decaying tops [40, 68] and 640 GeV when considering semi-leptonic decaying tops [67, 69]. Both searches are heavily rely on the energetic top quarks to suppress the huge $t\bar{t}$ background, so they will immediately loose the sensitivity when the LSP mass goes up to ~ 300 GeV.

As mentioned in the Introduction, for gluino decaying into the first two-generation quarks and LSP, searches for final state with energetic jets and large missing energy [33] as well as final state with high jet multiplicity [6, 34, 36] will put very strong bounds on gluino mass. When gluino is decaying through the third generation squarks, the final states will

contain many b-jets and leptons. So, searches for multi-b-jets [35, 40, 70] and lepton plus multi-jets [38, 39] can constrain these channels. What is more, because gluino is Majorana particle, the same sign di-lepton (SSDL) may show up in the final state. The search for SSDL [37] can also impose strong constraint for gluino, especially when it decays through top squark.

We recast all those analyses closely following the method introduced in [25]. Events are generated by MadGraph5, where Pythia6 and PGS have been packed to implement parton shower, hadronization and detector simulation as above. In PGS, we take the b-tagging efficiency of 70%, with c-mistag and light-jet mis-tag rates of 20% and 10%, otherwise specified in corresponding analysis. The M_{T_2} variables in some of the analyses are calculated by Oxbridge Kinetics Library [71, 72]. By comparing the upper limit on number of new physics events in each signal region and the number of events given by our model, we can tell whether our model is excluded or not. And we define the R_{vis}^i to measure the exclusion potential

$$R_{\text{vis}}^i = \frac{\text{Number of events given by our model in signal region } i}{\text{Upper limit for new physics events in signal region } i}. \quad (32)$$

Among all the signal regions, we define

$$R_{\text{max}} = \text{Max}_i(R_{\text{vis}}^i), \quad i = \text{all signal regions} \quad (33)$$

Obviously, the model is excluded only if $R_{\text{max}} > 1$. It has to be noted that we are only using leading order sparticle production cross sections throughout the work. Thus, the R_{max} calculated in this study should be rescaled by the corresponding K-factor.

Because we have already scanned the viable parameter space in the heavy LSP MSSM with Higgs boson mass ~ 125 GeV, most of our models are in accord with the LHC searches. We propose four benchmark points (BP I, BP II, BP III, and BP IV) in Table 4 to have a closer look at the heavy LSP SUSY.

From Eq (22), the degree of fine-tuning grows dramatically with gluino mass. A gluino with mass larger than 1.9 TeV will produce more than the degree of fine-tuning 300. All four benchmark points are chosen such that gluino is not giving the largest fine-tuning. In other words, gluino is taken as light as possible. And then the maximal mixing in stop sector renders the \bar{A}_t always gives the largest fine-tuning. Moreover, a relatively light chargino is required to give large enough contributions to $(g-2)_\mu$. So, the LSP should be either wino-like or higgsino-like, and then the dark matter can have relatively large collision cross section with nucleons. The direct search for dark matter may easily exclude those points. However, the dark matter annihilation cross section is also considerable. So, the LSP relic abundance can be much lower than the observed value, which makes our LSP only a component of dark matters. As a result, we find all four benchmark points are safe for the LUX experiment while within the reach of the XENON1T experiment as shown in Fig 7.

BP I is the least fine-tuned model with $\Delta_Z = 161$ originating from \bar{A}_t . The gluino mass gives about 135 for degree of fine-tuning. And the relatively large μ contributes degree of fine-tuning of 153. All those parameters give rise to similar amount of fine-tuning. Because

Points	BP I	BP II	BP III	BP IV
$\tan\beta$	21.6	30.4	36.6	27.2
μ	796.1	603.1	504.7	594.9
M_A	1581.2	1499.4	1673.3	1444.6
\bar{M}_1	1806.1	2133.7	1838.9	1978.6
\bar{M}_2	798.4	973.8	796.3	1115.4
\bar{M}_3	445.1	545.8	550.3	413.3
\bar{A}_t	-1704.4	-2243.1	-2071.4	-2108.1
$\bar{m}_{L_{2,3}}$	459.6	770.2	872.0	451.8
$\bar{m}_{e_{2,3}}$	638.4	943.9	631.1	892.1
\bar{m}_{Q_3}	556.7	569.6	789.8	1012.6
\bar{m}_t	1195.0	1349.5	1483.8	1530.9
\bar{m}_b	1883.0	614.2	408.4	1652.6
\bar{A}_b	-16.5	-641.9	771.7	-676.4
\bar{m}_{Q_2}	2015.0	2232.7	2793.8	1887.3
m_{H_1}	127.0	124.1	126.7	124.1
m_{H_2}	1580.7	1499.0	1673.5	1444.4
m_A	1581.2	1499.4	1673.3	1444.6
m_{H^\pm}	1583.0	1501.4	1675.8	1446.9
$m_{\tilde{g}}$	1228.9	1341.1	1422.0	1095.1
$m_{\tilde{t}_1}$	754.1	661.0	717.0	845.4
$m_{\tilde{t}_2}$	1125.9	1046.5	1085.4	1120.3
$m_{\tilde{b}_1}$	799.2	755.8	792.8	932.7
$m_{\tilde{b}_2}$	2036.7	1100.2	936.5	1696.1

$m_{\tilde{\chi}_1^0}$	629.2	588.1	485.6	585.4
$m_{\tilde{\chi}_2^0}$	733.3	608.6	510.8	601.8
$m_{\tilde{\chi}_3^0}$	798.2	819.6	675.1	843.7
$m_{\tilde{\chi}_4^0}$	827.2	923.8	781.5	924.8
$m_{\tilde{\chi}_1^\pm}$	630.2	592.8	490.8	591.1
$m_{\tilde{\chi}_2^\pm}$	817.6	820.6	676.6	924.3
$m_{\tilde{s}_L}$	2272.3	2534.2	3025.0	2168.1
$m_{\tilde{s}_R}$	2227.2	2479.1	3005.4	2062.1
$m_{\tilde{\nu}_L}$	755.8	1023.8	969.2	920.1
$m_{\tilde{\mu}_L/\tilde{\mu}_L}$	759.8	1026.7	972.3	923.4
$m_{\tilde{\mu}_R/\tilde{\mu}_R}$	929.2	1278.1	1081.6	1147.3
$m_{\tilde{\nu}_\tau}$	720.9	954.4	831.6	865.0
$m_{\tilde{\tau}_1}$	722.1	956.2	804.6	867.1
$m_{\tilde{\tau}_2}$	874.0	1166.2	849.2	1058.4
$\text{Br}_{(B_s \rightarrow \mu^+ \mu^-)}/10^9$	3.35	4.31	4.53	3.65
Ωh^2	0.017	0.026	0.02	0.034
$\sigma_p^{SI} \text{ (pb)}/10^{-9}$	18.0	19.4	22.9	9.7
$(g-2)_\mu/10^{-10}$	5.27	5.67	8.65	5.17
$\text{Br}_{(\tilde{g} \rightarrow \tilde{t}_i t)}/(\%)$	44	51.4	44.2	34.2
$\text{Br}_{(\tilde{g} \rightarrow \tilde{b}_i b)}/(\%)$	56	48.6	55.8	65.8
$\text{Br}_{(\tilde{t} \rightarrow \tilde{\chi}_i^0 t)}/(\%)$	0	0	38.4	51.4
$\text{Br}_{(\tilde{t} \rightarrow \tilde{\chi}_i^\pm b)}/(\%)$	100	100	61.6	48.6
R_{max}	0.32	0.13	0.20	0.55
Δ_Z	161(\bar{A}_t)	279(\bar{A}_t)	238(\bar{A}_t)	247(\bar{A}_t)

Table 4: Four benchmark points for heavy LSP SUSY in the natural MSSM.

the gluino is relatively light for this point, a relatively heavy LSP is needed to ensure the safety from the LHC SUSY searches. We find $R_{\text{max}} = 0.32$ from searching final states with missing energy and at least three b-jets [35]. The gluino cascade decays into the LSP either through $\tilde{g} \rightarrow t\tilde{t}_1$ or $\tilde{g} \rightarrow b\tilde{b}$. The stop is 100% decaying into $\tilde{\chi}_1^\pm b$ where the light chargino is degenerate with wino-like LSP and can be effectively regarded as the LSP. The total energy scale can be estimated as

$$E \sim 2 \times \left(\frac{m_{\tilde{g}}}{2} \left(1 - \frac{m_{\tilde{t}/\tilde{b}}^2}{m_{\tilde{g}}^2} \right) + \frac{m_{\tilde{t}/\tilde{b}}}{2} \left(1 - \frac{m_{\text{LSP}}^2}{m_{\tilde{t}/\tilde{b}}^2} \right) \right) \sim 1 \text{ TeV} . \quad (34)$$

Thus, the effective mass cut ($m_{\text{eff}} \gtrsim 1 \text{ TeV}$) in Ref. [35] excludes a great amount of signal events.

The stop sector is relatively light in BP II. The large \bar{A}_t , which is required by the Higgs boson mass, gives the largest fine-tuning $\Delta_Z = 279$, and the gluino mass gives the second largest fine-tuning $F_{\bar{M}_3} = 202$. However, as discussed above, the heavy LSP ($\sim 600 \text{ GeV}$)

is far beyond the current reach (~ 300 GeV). So, there is basically no contribution from the light stop sector. Because of the heavier gluino in this point, the search [35] gives the $R_{\text{max}} = 0.13$, and the energy scale of the point is a little bit higher than BP I

$$E \sim 1.2 \text{ TeV} . \quad (35)$$

Due to the relatively light higgsino LSP in BP III, the muon anomalous magnetic moment can be greatly enhanced. As the energy scale of final states at the LHC increases quadratically with decreasing LSP mass, the gluino mass should be further lifted to evade the search constraints. The sparticle production cross sections at the LHC are dominant by the stop and sbottom pairs. And the search for final states with missing energy and two b-jets [70] gives $R_{\text{max}} = 0.2$. The energy scale of this point is around

$$E \sim 1.5 \text{ TeV} , \quad (36)$$

which is significantly higher than BP II. Thus, its discovery potential is higher than BP II, even with heavier sparticles, e.g., gluino, stop and sbottom. Again, \bar{A}_t and \bar{M}_3 give the largest degree of fine-tuning, which are 238 and 206, respectively.

Finally, BP IV shows the most remarkable feature of the heavy LSP SUSY, whose gluino is very light (1095 GeV) while the LSP mass is heavy (585.4 GeV). Since stop and sbottom are heavy for this benchmark point, the LHC searches constrain the gluino mass most. The corresponding gluino production energy scale is

$$E \sim 900 \text{ GeV} . \quad (37)$$

So, the light gluino can still survive the current searches. The most sensitive analysis is still the search for final states with missing transverse energy and at least three b-jets [35], which gives $R_{\text{max}} = 0.55$. However, \bar{A}_t is relatively large for this benchmark point, which render this point suffering from the large degree of fine-tuning ~ 247 .

6 Discussions and Conclusion

We have proposed the heavy LSP SUSY, which can escape the LHC SUSY search constraints while preserve the naturalness in the MSSM. Interestingly, all the other experimental constraints can be satisfied as well. To understand why the heavy LSP SUSY can avoid the LHC bounds, we have presented the detailed kinematic analyses both analytically and numerically. An energy scale measure P was introduced to show the typical energy scale of a process. The E_T^{miss} and H_T are proportional to P with some coefficients depending on the decay modes. By assuming their distributions, we can naively estimate the cut efficiencies for experimental analyses. Thus, we have explicitly shown how the heavy LSP SUSY does work. What is more, the corresponding exclusion bounds can be roughly reproduced.

In addition, we have considered the naturalness problem for the heavy LSP SUSY in the MSSM. Using the Barbieri-Giudice fine-tuning measure, we studied the degree of fine-tuning produced by the GUT-scale parameters in details. We found that in the MSSM the Higgs

boson mass requirement is always the dominant source of fine-tuning and then the presence of heavy LSP will not introduce any more fine-tuning.

To realize the heavy LSP SUSY in the natural MSSM, we have scanned the viable parameter space. Based on the collider search sensitivity, we proposed four benchmark points to illustrate the heavy LSP SUSY. For these benchmark points, \bar{A}_t always gives the largest fine-tuning, as expected from the stop contributions to Higgs boson mass. And gluino can be as light as 1.1 TeV with $m_{\text{LSP}} \sim 600$ GeV while keep undetected by all the LHC SUSY searches. Meanwhile, the existence of light wino or higgsino can explain the $(g-2)_\mu$ excess within 3σ level.

Even though the total energy scale decreases quadratically with increasing LSP mass, some of the cuts are not so sensitive to it. This is the main reason why the multi-b tagging tends to give the most stringent bounds in most cases. Other cuts like M_{T2} only decrease linearly with the LSP mass, so the searches using M_{T2} etc are weaker than those using H_T or m_{eff} . How to search for the heavy LSP SUSY at the 14 TeV LHC is an interesting question, and we will leave it for a future work.

Acknowledgements

This work is supported in part by the Natural Science Foundation of China under grant numbers 10821504, 11075194, 11135003, and 11275246, and by the National Basic Research Program of China (973 Program) under grant number 2010CB833000.

References

- [1] **ATLAS Collaboration** Collaboration, G. Aad *et al.*, “Observation of a new particle in the search for the Standard Model Higgs boson with the ATLAS detector at the LHC,” *Phys.Lett.* **B716** (2012) 1–29, 1207.7214.
- [2] **CMS Collaboration** Collaboration, S. Chatrchyan *et al.*, “Observation of a new boson at a mass of 125 GeV with the CMS experiment at the LHC,” *Phys.Lett.* **B716** (2012) 30–61, 1207.7235.
- [3] H. P. Nilles, “Supersymmetry, Supergravity and Particle Physics,” *Phys.Rept.* **110** (1984) 1–162.
- [4] H. E. Haber and G. L. Kane, “The Search for Supersymmetry: Probing Physics Beyond the Standard Model,” *Phys.Rept.* **117** (1985) 75–263.
- [5] S. P. Martin, “A Supersymmetry primer,” hep-ph/9709356.
- [6] **CMS Collaboration** Collaboration, S. Chatrchyan *et al.*, “Search for gluino mediated bottom- and top-squark production in multijet final states in pp collisions at 8 TeV,” *Phys.Lett.* **B725** (2013) 243–270, 1305.2390.

- [7] **ATLAS Collaboration** Collaboration, G. Aad *et al.*, “Search for squarks and gluinos with the ATLAS detector in final states with jets and missing transverse momentum using $\sqrt{s} = 8$ TeV proton–proton collision data,” 1405.7875.
- [8] <https://twiki.cern.ch/twiki/bin/view/AtlasPublic/SupersymmetryPublicResults>
<https://twiki.cern.ch/twiki/bin/view/CMSPublic/PhysicsResultsSUS>.
- [9] M. Bastero-Gil, C. Hugonie, S. King, D. Roy, and S. Vempati, “Does LEP prefer the NMSSM?,” *Phys.Lett.* **B489** (2000) 359–366, hep-ph/0006198.
- [10] F. Bazzocchi and M. Fabbrichesi, “Little hierarchy problem for new physics just beyond the LHC,” *Phys.Rev.* **D87** (2013), no. 3, 036001, 1212.5065.
- [11] M. Papucci, J. T. Ruderman, and A. Weiler, “Natural SUSY Endures,” *JHEP* **1209** (2012) 035, 1110.6926.
- [12] C. Balazs, M. S. Carena, A. Freitas, and C. Wagner, “Phenomenology of the nMSSM from colliders to cosmology,” *JHEP* **0706** (2007) 066, 0705.0431.
- [13] U. Ellwanger, C. Hugonie, and A. M. Teixeira, “The Next-to-Minimal Supersymmetric Standard Model,” *Phys.Rept.* **496** (2010) 1–77, 0910.1785.
- [14] J. Espinosa and M. Quiros, “Higgs triplets in the supersymmetric standard model,” *Nucl.Phys.* **B384** (1992) 113–146.
- [15] O. Felix-Beltran, “Higgs masses and coupling within an extension of the MSSM with Higgs triplets,” *Int.J.Mod.Phys.* **A17** (2002) 465–486.
- [16] S. Di Chiara and K. Hsieh, “Triplet Extended Supersymmetric Standard Model,” *Phys.Rev.* **D78** (2008) 055016, 0805.2623.
- [17] R. Barbier, C. Berat, M. Besancon, M. Chemtob, A. Deandrea, *et al.*, “R-parity violating supersymmetry,” *Phys.Rept.* **420** (2005) 1–202, hep-ph/0406039.
- [18] **ATLAS Collaboration** Collaboration, G. Aad *et al.*, “Search for supersymmetry in events with four or more leptons in $\sqrt{s} = 8$ TeV pp collisions with the ATLAS detector,” 1405.5086.
- [19] **CMS Collaboration** Collaboration, Tech. Rep. CMS-PAS-SUS-13-010, CERN, Geneva, 2013.
- [20] T. J. LeCompte and S. P. Martin, “Large Hadron Collider reach for supersymmetric models with compressed mass spectra,” *Phys.Rev.* **D84** (2011) 015004, 1105.4304.
- [21] T. J. LeCompte and S. P. Martin, “Compressed supersymmetry after 1/fb at the Large Hadron Collider,” *Phys.Rev.* **D85** (2012) 035023, 1111.6897.

- [22] M. A. Ajaib, T. Li, and Q. Shafi, “Stop-Neutralino Coannihilation in the Light of LHC,” *Phys.Rev.* **D85** (2012) 055021, 1111.4467.
- [23] X.-J. Bi, Q.-S. Yan, and P.-F. Yin, “Probing Light Stop Pairs at the LHC,” *Phys.Rev.* **D85** (2012) 035005, 1111.2250.
- [24] E. Alvarez and Y. Bai, “Reach the Bottom Line of the Sbottom Search,” *JHEP* **1208** (2012) 003, 1204.5182.
- [25] T. Cheng, J. Li, T. Li, and Q.-S. Yan, “Natural NMSSM confronting with the LHC7-8,” *Phys.Rev.* **D89** (2014) 015015, 1304.3182.
- [26] C. Han, A. Kobakhidze, N. Liu, A. Saavedra, L. Wu, *et al.*, “Probing Light Higgsinos in Natural SUSY from Monojet Signals at the LHC,” *JHEP* **1402** (2014) 049, 1310.4274.
- [27] Z. Han, G. D. Kribs, A. Martin, and A. Menon, “Hunting quasidegenerate Higgsinos,” *Phys.Rev.* **D89** (2014) 075007, 1401.1235.
- [28] P. W. Graham, D. E. Kaplan, S. Rajendran, and P. Saraswat, “Displaced Supersymmetry,” *JHEP* **1207** (2012) 149, 1204.6038.
- [29] J. Fan, M. Reece, and J. T. Ruderman, “Stealth Supersymmetry,” *JHEP* **1111** (2011) 012, 1105.5135.
- [30] J. Guo, Z. Kang, J. Li, T. Li, and Y. Liu, “Simplified Supersymmetry with Sneutrino LSP at 8 TeV LHC,” 1312.2821.
- [31] D. S. M. Alves, J. Liu, and N. Weiner, “Hiding Missing Energy in Missing Energy,” 1312.4965.
- [32] F. Brummer, S. Kraml, and S. Kulkarni, “Anatomy of maximal stop mixing in the MSSM,” *JHEP* **1208** (2012) 089, 1204.5977.
- [33] T. A. collaboration, “Search for squarks and gluinos with the ATLAS detector in final states with jets and missing transverse momentum and 20.3 fb⁻¹ of $\sqrt{s} = 8$ TeV proton-proton collision data,”.
- [34] **CMS Collaboration** Collaboration, S. Chatrchyan *et al.*, “Search for new physics in the multijet and missing transverse momentum final state in proton-proton collisions at $\sqrt{s} = 8$ TeV,” 1402.4770.
- [35] T. A. collaboration, “Search for strong production of supersymmetric particles in final states with missing transverse momentum and at least three b-jets using 20.1 fb1 of pp collisions at $\sqrt{s} = 8$ TeV with the ATLAS Detector.,”.

- [36] **ATLAS Collaboration** Collaboration, G. Aad *et al.*, “Search for new phenomena in final states with large jet multiplicities and missing transverse momentum at $\sqrt{s}=8$ TeV proton-proton collisions using the ATLAS experiment,” *JHEP* **1310** (2013) 130, 1308.1841.
- [37] **CMS Collaboration** Collaboration, C. Collaboration, “Search for new physics in events with same-sign dileptons and jets in pp collisions at 8 TeV,”.
- [38] **CMS Collaboration** Collaboration, C. Collaboration, “Search for supersymmetry in pp collisions at $\sqrt{s} = 8$ TeV in events with three leptons and at least one b-tagged jet,”.
- [39] **CMS Collaboration** Collaboration, S. Chatrchyan *et al.*, “Search for supersymmetry in pp collisions at $\sqrt{s}=8$ TeV in events with a single lepton, large jet multiplicity, and multiple b jets,” *Phys.Lett.* **B733** (2014) 328–353, 1311.4937.
- [40] **CMS Collaboration** Collaboration, C. Collaboration, “Search for supersymmetry using razor variables in events with b-jets in pp collisions at 8 TeV,”.
- [41] B. L. Roberts, “Status of the Fermilab Muon ($g - 2$) Experiment,” *Chin.Phys.* **C34** (2010) 741–744, 1001.2898.
- [42] J. Alwall, M. Herquet, F. Maltoni, O. Mattelaer, and T. Stelzer, “MadGraph 5 : Going Beyond,” *JHEP* **1106** (2011) 128, 1106.0522.
- [43] T. Sjostrand, S. Mrenna, and P. Z. Skands, “PYTHIA 6.4 Physics and Manual,” *JHEP* **0605** (2006) 026, hep-ph/0603175.
- [44] J. Conway,
“<http://www.physics.ucdavis.edu/~conway/research/software/pgs/pgs4-general.htm>,”.
- [45] **CMS Collaboration** Collaboration, Tech. Rep. CMS-PAS-SUS-13-015, CERN, Geneva, 2013.
- [46] J. R. Ellis, K. Enqvist, D. V. Nanopoulos, and F. Zwirner, “Observables in Low-Energy Superstring Models,” *Mod.Phys.Lett.* **A1** (1986) 57.
- [47] R. Barbieri and G. Giudice, “Upper Bounds on Supersymmetric Particle Masses,” *Nucl.Phys.* **B306** (1988) 63.
- [48] L. E. Ibanez, C. Lopez, and C. Munoz, “The Low-Energy Supersymmetric Spectrum According to N=1 Supergravity Guts,” *Nucl.Phys.* **B256** (1985) 218–252.
- [49] A. Lleyda and C. Munoz, “Nonuniversal soft scalar masses in supersymmetric theories,” *Phys.Lett.* **B317** (1993) 82–91, hep-ph/9308208.
- [50] H. Abe, T. Kobayashi, and Y. Omura, “Relaxed fine-tuning in models with non-universal gaugino masses,” *Phys.Rev.* **D76** (2007) 015002, hep-ph/0703044.

- [51] J. L. Feng, “Naturalness and the Status of Supersymmetry,” *Ann.Rev.Nucl.Part.Sci.* **63** (2013) 351–382, 1302.6587.
- [52] H. Baer, V. Barger, D. Mickelson, and M. Padeffke-Kirkland, “SUSY models under siege: LHC constraints and electroweak fine-tuning,” 1404.2277.
- [53] F. Jegerlehner, “Essentials of the Muon $g-2$,” *Acta Phys.Polon.* **B38** (2007) 3021, hep-ph/0703125.
- [54] J. Bijnens and J. Prades, “The Hadronic Light-by-Light Contribution to the Muon Anomalous Magnetic Moment: Where do we stand?,” *Mod.Phys.Lett.* **A22** (2007) 767–782, hep-ph/0702170.
- [55] A. Czarnecki, W. J. Marciano, and A. Vainshtein, “Refinements in electroweak contributions to the muon anomalous magnetic moment,” *Phys.Rev.* **D67** (2003) 073006, hep-ph/0212229.
- [56] K. Hagiwara, R. Liao, A. D. Martin, D. Nomura, and T. Teubner, “ $(g - 2)_\mu$ and $\alpha(M_Z^2)$ re-evaluated using new precise data,” *J.Phys.* **G38** (2011) 085003, 1105.3149.
- [57] **LHCb Collaboration** Collaboration, R. Aaij *et al.*, “First Evidence for the Decay $B_s^0 \rightarrow \mu^+ \mu^-$,” *Phys.Rev.Lett.* **110** (2013) 021801, 1211.2674.
- [58] A. Djouadi, J.-L. Kneur, and G. Moultaka, “SuSpect: A Fortran code for the supersymmetric and Higgs particle spectrum in the MSSM,” *Comput.Phys.Commun.* **176** (2007) 426–455, hep-ph/0211331.
- [59] G. Belanger, F. Boudjema, A. Pukhov, and A. Semenov, “micrOMEGAs: Version 1.3,” *Comput.Phys.Commun.* **174** (2006) 577–604, hep-ph/0405253.
- [60] G. Belanger, F. Boudjema, A. Pukhov, and A. Semenov, “micrOMEGAs3: A program for calculating dark matter observables,” *Comput.Phys.Commun.* **185** (2014) 960–985, 1305.0237.
- [61] G.-C. Cho, K. Hagiwara, Y. Matsumoto, and D. Nomura, “The MSSM confronts the precision electroweak data and the muon $g-2$,” *JHEP* **1111** (2011) 068, 1104.1769.
- [62] **Planck Collaboration** Collaboration, P. Ade *et al.*, “Planck 2013 results. XVI. Cosmological parameters,” 1303.5076.
- [63] **LUX Collaboration** Collaboration, D. Akerib *et al.*, “First results from the LUX dark matter experiment at the Sanford Underground Research Facility,” *Phys.Rev.Lett.* **112** (2014) 091303, 1310.8214.
- [64] **XENON1T collaboration** Collaboration, E. Aprile, “The XENON1T Dark Matter Search Experiment,” 1206.6288.

- [65] **ATLAS Collaboration**, G. Aad *et al.*, “Search for direct third-generation squark pair production in final states with missing transverse momentum and two b -jets in $\sqrt{s} = 8$ TeV pp collisions with the ATLAS detector,” *JHEP* **1310** (2013) 189, 1308.2631.
- [66] **ATLAS Collaboration**, G. Aad *et al.*, “Search for direct top-squark pair production in final states with two leptons in pp collisions at $\sqrt{s}=8$ TeV with the ATLAS detector,” 1403.4853.
- [67] **CMS Collaboration**, S. Chatrchyan *et al.*, “Search for top-squark pair production in the single-lepton final state in pp collisions at $\sqrt{s} = 8$ TeV,” *Eur.Phys.J.* **C73** (2013) 2677, 1308.1586.
- [68] **ATLAS Collaboration**, “Search for direct production of the top squark in the all-hadronic $t\bar{t}b\bar{b}$ + \cancel{E}_T final state in 21 fb-1 of p - p collisions at $\sqrt{s}=8$ TeV with the ATLAS detector,”.
- [69] **ATLAS Collaboration**, “Search for direct top squark pair production in final states with one isolated lepton, jets, and missing transverse momentum in $\sqrt{s} = 8$, TeV pp collisions using 21 fb $^{-1}$ of ATLAS data,”.
- [70] **ATLAS Collaboration**, “Search for direct sbottom production in event with two b -jets using 12.8 fb-1 of pp collisions at $\sqrt{s} = 8$ TeV with the ATLAS Detector.,”.
- [71] C. Lester and D. Summers, “Measuring masses of semiinvisibly decaying particles pair produced at hadron colliders,” *Phys.Lett.* **B463** (1999) 99–103, hep-ph/9906349.
- [72] A. Barr, C. Lester, and P. Stephens, “ $m(T_2)$: The Truth behind the glamour,” *J.Phys.* **G29** (2003) 2343–2363, hep-ph/0304226.